Enhancing Drivers' Perception of Traffic Lights through Haptic Alerts on the Brake Pedal

1st Chanyeong Jeong
Automotive Materials & Component
Korea Institute of Industrial Technology
Gwangju, South Korea
egkim@kitech.re.kr

2nd Eugene Kim
Automotive Materials & Component
Korea Institute of Industrial Technology
Gwangju, South Korea
egkim@kitech.re.kr

3rd Myeong-Hwan Hwang
Automotive Materials & Component
Korea Institute of Industrial Technology
Gwangju, South Korea
han9215@kitech.re.kr

4th Hyun-Rok Cha
Automotive Materials & Component
Korea Institute of Industrial Technology
Gwangju, South Korea
hrcha@kitech.re.kr

***Abstract*—In recent times, the increase in traffic volume has led to concerns regarding traffic congestion and safety issues. Various approaches utilizing roadway infrastructure and vehicle systems have been proposed to address these challenges. In this context, we focused on human-machine interfaces that can provide direct signals to humans. Haptic alerts have been extensively studied using feedback mechanisms such as steering wheels or seats, and previous research on pedal haptics has primarily aimed at improving safety. However, to the best of the authors' knowledge, there is a lack of research specifically investigating driver responses when pedal haptic feedback is provided. We propose a novel approach utilizing a motor in the integrated brake system as a feedback method. Our study aims to investigate the promise of haptic alerts on the brake pedal method. Haptic alerts are generated using a motor that activates the integrated brake system, producing waves with specific frequency and amplitude. Using this approach, an simulation on haptic alerts on the brake pedal was conducted, evaluating the position command followability of haptic alerts. The records were obtained by simulating the position control of a three-phase motor for haptic command waveforms with combinations of preset frequencies and amplitudes. The results indicate that haptic alert requires the appropriate frequencies and amplitudes under the performance limits of the system. As part of our future work, we plan to conduct experiments on external environment perception among drivers and evaluate the impact of haptic alerts. Furthermore, we intend to present haptic alert waves with various frequencies and amplitudes to measure the resulting changes in driver response.**

***Index Terms*—Haptic, Integrated Brake System, Traffic**

I. Introduction

Recent studies are focused on haptic systems for enhancement of stability and mobility of the vehicle [1]. As for the nominal case of the enhancement of the human driver's perception, the haptic system is included for the steering wheel or a driver's seat [2], [3]. However, costs arise for the design of the structure or system in order to additionally induce vibration. In the real case scenario, it is unnecessary to provide sensitive/powerful haptic systems. Therefore, in the case of using it just for reminding the driver, the basically-mounted haptic function can be utilized. Among the pedal system, especially the brake system for instance, EHB (Electro-hydraulic Brake) and EMB (Electro-mechanical Brake), the brake-by-wire system can control the brake pedal without the human driver's action [4]. In this study, implementing a haptic alert system to the brake pedal was discussed.

There are various types of applying haptic systems to the gas pedals [5], [6]. Upper mentioned articles focus on the car-following and applied with gas pedals, not the basically mounted brake systems. On the other hand, neuro-muscle analysis was taken out to estimate the driver's physical condition not only the pedal haptic control [7]. However, this research focuses on the enhancement of environmental cognition not the actual state of the driver. Also, several researches were conducted to investigate the effect of the haptic system applied to the regenerative brake system [8]. In addition, the economic driving cognition function was investigated [9]. However, by far of the author's knowledge, the brake haptic system focusing on the alert system of the environmental situation was not reported.

In this study, the following effect is anticipated by the use of the proposed system. Firstly, it can aid the enhancement of the driver's mobility by recognizing the environmental situations. Secondly, reducing the design cost of the haptic feedback system since it does not require any additional motor or structure modifications.

II. Methodology

In this section, the methodology of electro-mechanical brake control is shown.

This study has been conducted with the support of the Korea Institute of Industrial Technology as "Development of Core Technologies for a Working Partner Robot in the Manufacturing Field"(KITECH EO-23-0009)

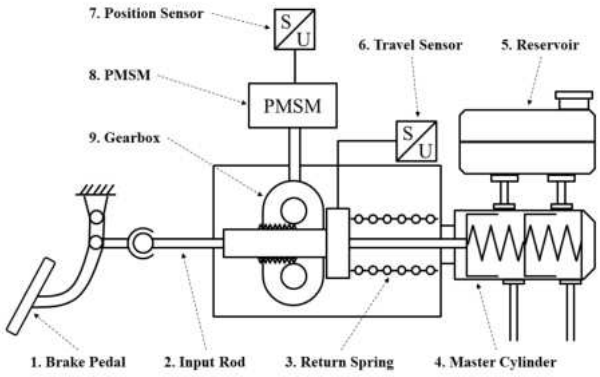

Fig. 1. An example structure of Electro-mechanical brake. Without a vacuum brake booster, PMSM (Permanent Magnet Synchronous Motor) assists the power of the driver's pedal load, or it is a structure that can automatically operate the brake under the control of PMSM.

A. Electro-mechanical brake structure

The structure of the electro-mechanical brake is shown in Fig. 1. The brake pedal is connected to the input rod, and the travel sensor measures the linear position of the input rod. The input rod compresses the inside of the master cylinder and transmits hydraulic pressure to each wheel. In addition, the input rod meshes with the gearbox composed of special worm/worm gear and reduction gear and is connected to the PMSM, and translates linearly according to the rotation of the PMSM. In fact, the linear translation of the input rod is proportional to the rotational position of the PMSM. Therefore, in the brake system with the structure of Fig. 1, the brake pedal can be moved through the control of PMSM. Using this characteristic, a haptic system can be implemented on the brake pedal.

B. Motor control

The PMSM is operated by supplying 3-phase current, and time varying differential equation analyzes are required for individual control of each phase. In order to solve the complexity, Clarke and Park transformation is introduced to convert three phases into two axes, d-axis and q-axis [10]. For example, when the three-phase currents supplied to the motor are obtained for feedback, the measured value is converted into dq-axes-based variables by Clarke and Park transformation during the control operation. Conversely, the demand voltages that were calculated based on the dq-axes are supplied to the motor in three phases by inverse Clarke and Park transformation.

Field-oriented control is a method of controlling a 3-phase PMSM. A simplified control loop is introduced in Fig. 2.

In the inner loop, the outputs of current PI controller for the d-axis and q-axis are applied with the inverse Clarke and Park transformation. After the transformation, the 3-phase outputs are converted to demand voltage through SVPWM (Space Vector Pulse Width Modulation) technique. The 3-phase demand voltages are finally generated by PWM (Pulse Width Modulation) in devices such as FET (Field Effect Transistor). In the intermediate loop and the outer loop, each PI controller receives the demand position and the demand velocity and outputs the demand target for the loop inside. The present rotational incremental counter and sector of the motor are obtained by hall sensors and encoders mounted on PMSM. The angle and the angular velocity of the motor are calculated with sensor data and used in position or velocity feedbacks and the Clarke and Park transformation. In the motor controller circuit, the current for each three phases are measured and fed back in the current controller.

In this study, because control methods using the d-axis such as MTPA (Maximum Torque Per Ampere) or flux weakening control are not used, the demand voltage for d-axis V_d is always set to zero. The torque and voltage equations of an surface mounted PMSM for q-axis is shown in (2):

$$T = \frac{3}{2}\frac{p}{2}\lambda_f i_q \tag{1}$$

$$V_q = R\ i_q + \omega_e L i_d + L\frac{\mathrm{d}i_q}{\mathrm{d}t} + \omega_e \lambda_f \tag{2}$$

where T is the torque, p is the number of poles, L is the inductance, i_d and i_q are the current for each axis, λ_f is the field flux caused by the permanent magnet, V_q is the voltage for q-axis, R is the resistance of the stator, and ω_e is the electrical angular velocity [10].

III. Simulation

A. Haptic brake system settings

The Haptic Brake System (HBS) for the experiment is configured with the EMB, EMB controller, and EMB jig as described in Fig. 3.

The model iBooster of Bosch which is built in electric vehicles of Chevrolet and Tesla is used for EMB. The EMB is fixed at the EMB jig, and offers signals from internal travel sensor to the controller. The controller acquires 3-phased hall signals and two encoder signals from magnetic rotary position sensor named AS5147P. Haptic signals are transmitted to the brake pedal from the EMB controller.

B. Simulation

The haptic performance of the EMB was first verified by MATLAB simulations prior to conducting the experiment with subjects. Specifications of a virtual motor in the simulation were set to measured and estimated values of the 3-phase motor in the HBS. Parameters, symbols, and values used in the simulation are introduced in Table I.

The haptic signal was the form of square waves with various frequencies and amplitudes. In the real environment, a square wave is preferred instead of a sinusoidal wave because the controller has limited computing power. Therefore, the square wave was used in the simulation. The haptic command waveform design conditions for amplitudes and frequencies are $(0.5, 1.0, 1.5, 2.0, 2.5, 3.0)$ millimeters and $(10, 7.5, 5, 2.5)$ hertz each.

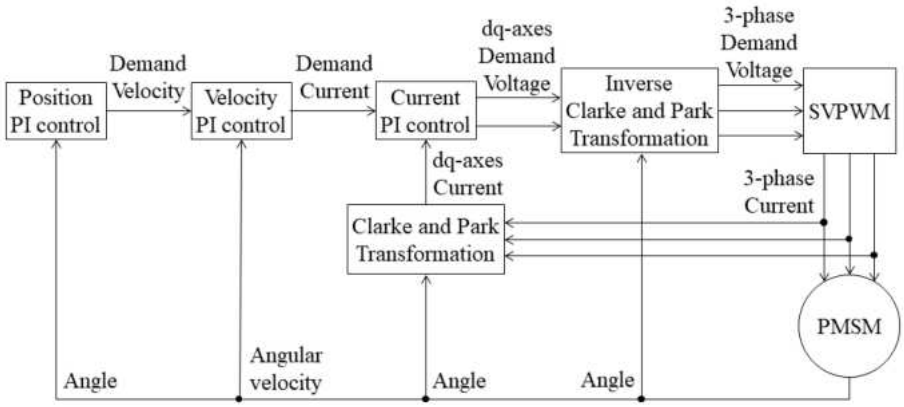

Fig. 2. The cascade controller for PMSM. Inner loop for the current control and voltage control, an intermediate loop for the velocity control, and an outer loop for the position control.

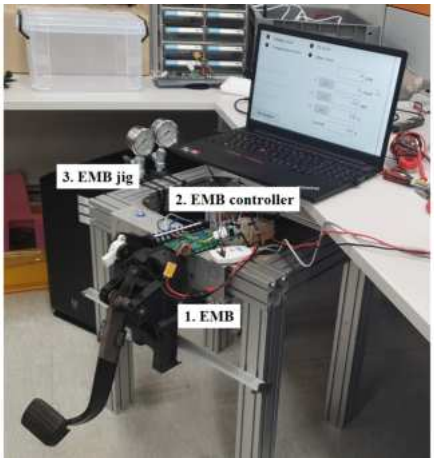

Fig. 3. The experimental hardware for pedal haptic function.

TABLE I
SELECTED MOTOR SPECIFICATION FOR SIMULATION.

Parameter	Symbol	Value
Rated Voltage	V_r	12 V
Rated Velocity	ω_r	1920 RPM
Rated Torque	T_r	1.58 N·m
Power	P	316 W
Poles	p	14
Resistance	R	0.448 Ω
Inductance	L	0.165 mH
Moment of Inertia	J	0.0047 N·m^2
Motor to Linear Ratio	ρ	0.4 mm/rad
Voltage Constant	K_e	0.12 V·s/rad
Torque Constant	K_t	0.1 N·m/A

The structure of the simulation is three-staged cascade PID controllers as shown in Fig. 2. PID gains were empirically chosen for each controller (Table II).

In order to ensure the control performance, control periods of each loop are different: 4000 hertz for the current controller, 1000 hertz for the velocity controller, and 250 hertz for the position controller. The simulation was conducted for 1 second while giving a haptic command.

TABLE II
PID GAINS FOR PI AND PID CONTROLLERS.

Controller	Gain	Value
Current	P	0.485
Current	I	0.5
Velocity	P	1.2
Velocity	I	0.12
Position	P	20
Position	I	0.01
Position	D	200

IV. RESULTS AND DISCUSSION

In this section, the simulation results according to various amplitudes and frequencies are presented. Firstly, the comparison of waveforms are offered. Next, the position control results for square waves are also presented.

A. Comparison of waveforms

Demand positions from haptic command waveform and position control outputs for sinusoidal and non-sinusoidal waves are presented in Fig. 4 and Fig. 5.

Fig. 5 suggests the fact that the periodic haptic command waveform causes the position control output to oscillate regardless of its shape. The phase, amplitude, and shape are slightly different for each output waveform, which is thought to be due to different followability. Unlike a sinusoidal wave, a triangular wave has a non-differentiable point. Also, the square wave consists of step inputs rather than ramp inputs of the triangle wave. From the morphological characteristics of the haptic command waveform, the influence on the vibration characteristics can be confirmed.

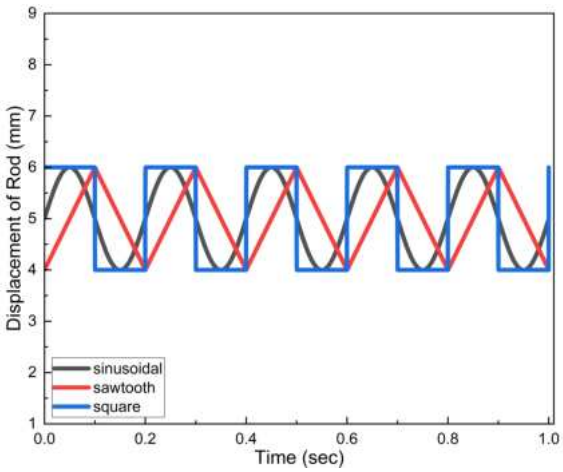

Fig. 4. Demand position of each waveform (1 mm amplitude and 5 Hz frequency for all).

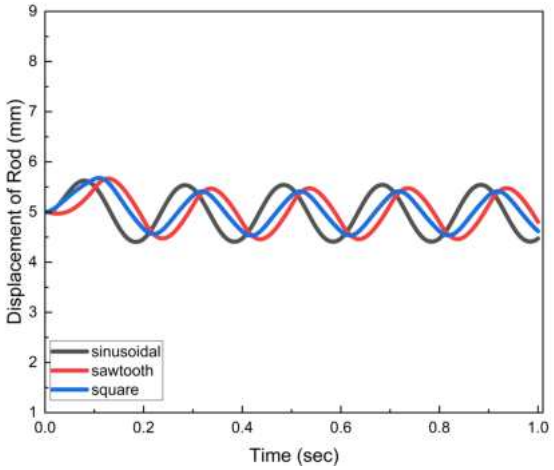

Fig. 5. Simulated outputs by the position control command in each waveform (1 mm amplitude and 5 Hz frequency for all).

B. Comparison of wave parameters

The simulation results of position control for demand waveforms are presented in Fig. 6, Fig. 7, Fig. 8, Fig. 9, Fig. 10, Fig. 11.

For a demand position of the same amplitude, as the frequency increases, the amplitude of the position control output gradually decreases. For example, in the case of 10 hertz, the amplitude of the position control output was decreased to 10-20% of the demand position. The decrease in position control output seems to arise due to the transition in demand position occurs as often as the speed of the frequency. However, even if the followability of the demand position is low, there is a possibility that the subject's senses can detect the vibration in the experiment. It is requisite to obtain a range of frequencies in which the subject feels the haptic through future experiments.

In the large amplitude region, a bias from the center point of the vibration that varies with time is identified in the position control output. Also, as the frequency increases, the bias also

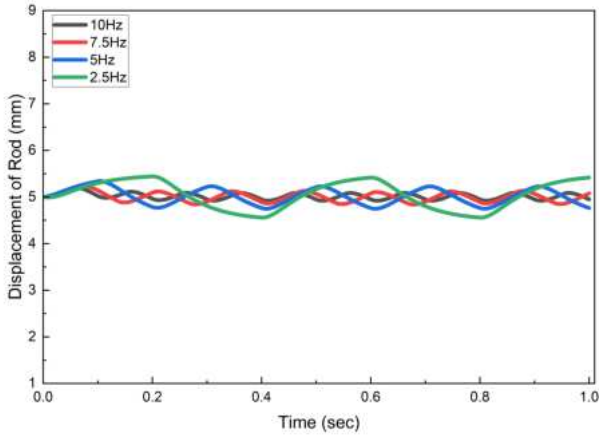

Fig. 6. Simulated outputs by the position control command in each frequencies (0.5 mm amplitude for all).

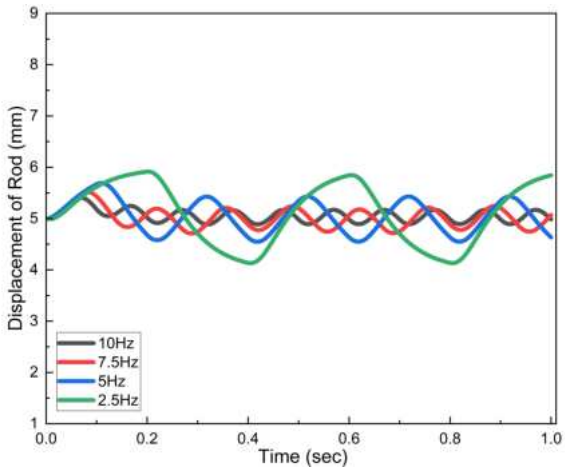

Fig. 7. Simulated outputs by the position control command in each frequencies (1 mm amplitude for all).

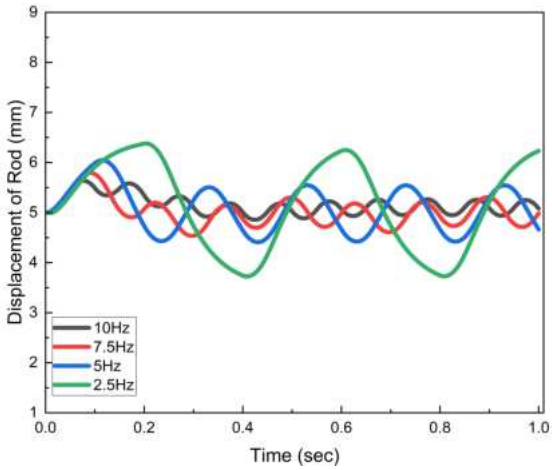

Fig. 8. Simulated outputs by the position control command in each frequencies (1.5 mm amplitude for all).

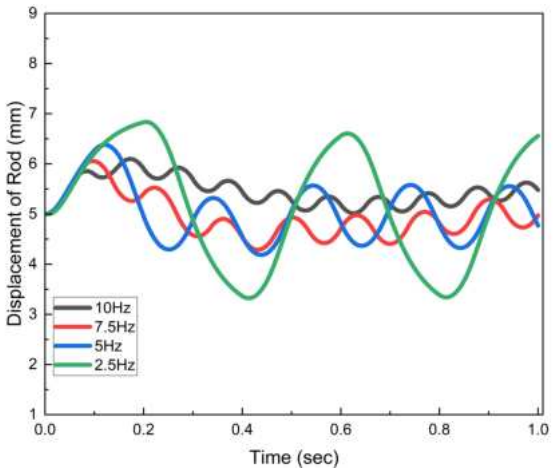

Fig. 9. Simulated outputs by the position control command in each frequencies (2 mm amplitude for all).

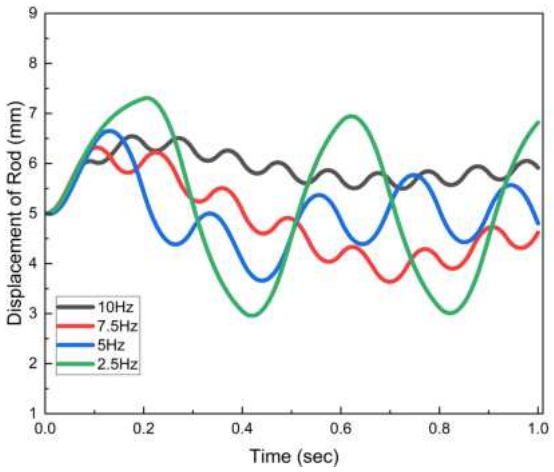

Fig. 10. Simulated outputs by the position control command in each frequencies (2.5 mm amplitude for all).

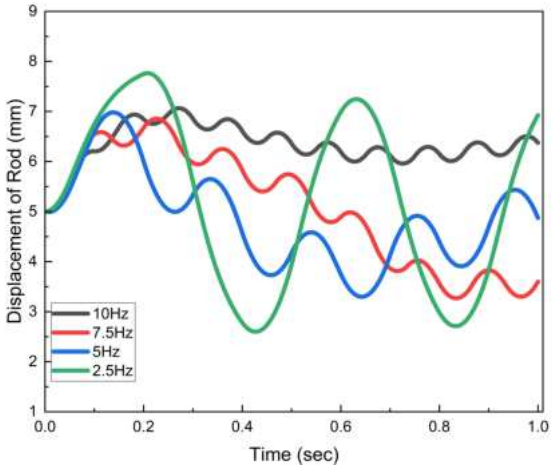

Fig. 11. Simulated outputs by the position control command in each frequencies (3 mm amplitude for all).

tends to increase. It is required to consider the amplitude for the experiment, and it is also necessary to experiment whether the subject feels a sense of heterogeneity for the changing center point of the vibration.

In conclusion, the range of frequency and amplitude is restricted due to the performance limitations of the motor set in the simulation. Moreover, not only motors but also EMB controllers have limitations in current input and output. Therefore, increasing controller performance is the main point of improvement. For a fast reaction rate, flux weakening control is required for extending the maximum velocity. MTPA technique also expected to overcome the maximum current limit. In addition, methods to increase the position followability to predictable haptic commands can be adopted. If only the embedded haptic waveform is provided without changing the waveform, using a predefined map for the waveform will provide good performance.

V. Conclusion

Our research introduced a novel approach employing a motor integrated into the EMB to provide haptic feedback. The main objective was to investigate the prospect of motor-driven haptic alerts. By generating haptic alerts with predefined frequencies and amplitudes, we conducted simulations to evaluate the performance of motor control for periodic position command. The results revealed the importance of using appropriate frequencies and amplitudes within the system's performance limits to achieve optimal haptic alert outcomes.

The future work aims to conduct experiments with drivers and developed HBS. First of all, the driver's perception of the external environment and the effect of the haptic alarm will be evaluated. Later, we will proceed with analysis of various frequencies and amplitudes to specify the optimal haptic alarm.

Acknowledgement

This study has been conducted with the support of the Korea Institute of Industrial Technology as "Development of Core Technologies for a Working Partner Robot in the Manufacturing Field"(KITECH EO-23-0009)

References

[1] S. M. Petermeijer, D. A. Abbink, M. Mulder, and J. C. De Winter, "The effect of haptic support systems on driver performance: A literature survey," *IEEE transactions on haptics*, vol. 8, no. 4, pp. 467–479, 2015.

[2] M. Steele and R. B. Gillespie, "Shared control between human and machine: Using a haptic steering wheel to aid in land vehicle guidance," in *Proceedings of the human factors and ergonomics society annual meeting*, vol. 45, pp. 1671–1675, SAGE Publications Sage CA: Los Angeles, CA, 2001.

[3] Y. G. Ji, K. Lee, and W. Hwang, "Haptic perceptions in the vehicle seat," *Human Factors and Ergonomics in Manufacturing & Service Industries*, vol. 21, no. 3, pp. 305–325, 2011.

[4] X. Hua, J. Zeng, H. Li, J. Huang, M. Luo, X. Feng, H. Xiong, and W. Wu, "A review of automobile brake-by-wire control technology," *Processes*, vol. 11, no. 4, p. 994, 2023.

[5] M. Mulder, M. Mulder, M. M. van Paassen, and D. A. Abbink, "Haptic gas pedal feedback," *Ergonomics*, vol. 51, no. 11, pp. 1710–1720, 2008. PMID: 18941976.

[6] M. Mulder, D. A. Abbink, M. M. van Paassen, and M. Mulder, "Design of a haptic gas pedal for active car-following support," *IEEE Transactions on Intelligent Transportation Systems*, vol. 12, no. 1, pp. 268–279, 2011.

[7] D. Abbink, M. Mulder, F. van der Helm, M. Mulder, and E. Boer, "Measuring neuromuscular control dynamics during car following with continuous haptic feedback," *IEEE transactions on systems, man, and cybernetics. Part B, Cybernetics : a publication of the IEEE Systems, Man, and Cybernetics Society*, vol. 41, pp. 1239–49, 04 2011.

[8] U. Caliskan and V. Patoglu, "Efficacy of haptic pedal feel compensation on driving with regenerative braking," *IEEE Transactions on Haptics*, vol. 13, no. 1, pp. 175–182, 2020.

[9] S. A. Birrell, M. S. Young, and A. M. Weldon, "Vibrotactile pedals: provision of haptic feedback to support economical driving," *Ergonomics*, vol. 56, no. 2, pp. 282–292, 2013. PMID: 23419088.

[10] S.-K. Sul, *Control of Electric Machine Drive Systems*. Wiley-IEEE Press, 2011.